

This Document  
Reproduced From  
Best Available Copy

SECURITY CLASSIFICATION: UNCLASSIFIED

COMPONENTS



LABORATORIES

LAND LOCOMOTION LABORATORY

Report No. 8090

LL No. 83

Copy No.       

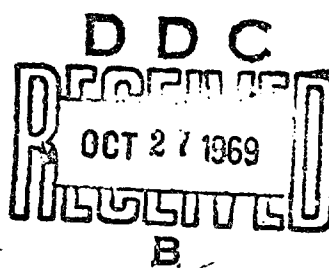
AD695669

PRESSURE DISTRIBUTION AND SLIP-SINKAGE RELATIONSHIP  
UNDER DRIVEN RIGID WHEELS

By

E. Hegedus

June, 1963



Project No: 5016.11.04400

Authenticated: Ronald A. Custer

D/A Project No: D/A 597-01-006

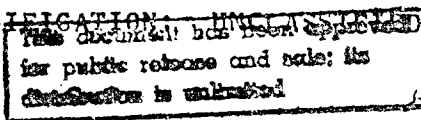
Approved: S. J. Zeller



U.S. ARMY TANK-AUTOMOTIVE CENTER  
CENTER LINE, MICHIGAN

Reproduced by the  
CLEARINGHOUSE  
for Federal Scientific & Technical  
Information Springfield Va. 22151

SECURITY CLASSIFICATION: UNCLASSIFIED



H7

### OBJECTIVE

Measure and analyze pressure distribution and slip sinkage relationships under rigid wheels in various types of soils.

### RESULTS

Pressure and slip-sinkage measurements for different wheel dimensions in five different types of soil are presented in chart form in such a way that the affect of slip, sinkage, soil properties, frictional forces, and wheel geometry on wheel behavior are clearly indicated.

### CONCLUSIONS

Sinkage, as well as pressure distribution, are a function of slip in granular soils. However, in the cohesive types of soils tested, both sinkage and pressure distribution were independent of slip.

Frictional forces must be included in wheel equilibrium equations if equilibrium is to be achieved.

### ADMINISTRATIVE INFORMATION

This program was supervised and conducted by the Land Locomotion Laboratory of ATAC, under D/A Project No. 597-01-006, Project No. 5016.11.34400.

## TABLE OF CONTENTS

	<u>Page No.</u>
Abstract . . . . .	iii
Acknowledgement . . . . .	iv
List of Figures . . . . .	v
Objective . . . . .	vii
Introduction . . . . .	1
Theoretical Background . . . . .	3
Test Facilities and Procedures . . . . .	5
Test Results . . . . .	9
Conclusions . . . . .	14
Recommendations . . . . .	15
References . . . . .	38

ABSTRACT

Normal pressure distribution and slip-sinkage relationships were studied experimentally under rigid wheels in various types of soil. The experiments were limited to driven wheels only; however, normal pressure distribution for a wide range of slip condition from 0 - 100% were obtained. Sinkage as well as pressure distribution was found to be dependent upon slip, soil properties, and wheel geometry in sand and in sandy loam with low moisture content, but in sandy loam with higher moisture content, sinkage and pressure distribution may be taken independent of slip. The analysis of data also revealed that the effects of frictional forces are significant and cannot be overlooked.

ACKNOWLEDGMENT

This report was prepared under the supervision of Mr. R. A. Liston, Chief of the Land Locomotion Laboratory, and Z. J. Janosi, Chief of the Theoretical Mechanics Section.

#### LIST OF FIGURES

##### Figure No.

1. Equilibrium of a Driven Wheel.
2. Test Apparatus.
3. Calibration of the Load Cells by Air Pressure.
4. Grain Size Distribution Diagram for Sand.
5. Torque as a Function of Slip with Load as Parameter in Dry Sand.
6. Normal Pressure Distribution for Different Wheel Loads in Sand at no Slip.
7. Effect of Wheel Slip on Pressure Distribution Under a 20 inch x 3 inch Wheel in Sand.
8. Effect of Wheel Slip on Pressure Distribution Under a 20 inch x 5 inch Wheel in Sand.
9. Lateral Pressure Distribution in Sand for Various Wheel Slips.
10. Sinkage as a Function of Slip for a 20 inch x 3 inch Wheel in Sand with Load as Parameter.
11. Sinkage as a Function of Slip for a 20 inch x 5 inch Wheel in Sand with Load as Parameter.
12. Sinkage as a Function of the Angle of Inclination of the Normal Reaction.
13. Equilibrium of the Vertical Forces for 20 inch x 3 inch Wheel in Dry Sand.
14. Sinkage as a Function of Slip for a 20 inch x 5 inch Wheel in Sandy-Loam at  $w = 4.9\%$  with Load as Parameter.

Figure No.

15. Sinkage as a Function of Slip for a 20 inch x 5 inch Wheel in Sandy-Loam at  $w = 6.5\%$  with Load as Parameter.
16. Sinkage as a Function of Slip for a 20 inch x 5 inch Wheel in Sandy-Loam at  $w = 9.1\%$  with Load as Parameter.
17. Sinkage as a Function of Slip for a 20 inch x 5 inch Wheel in Sandy-Loam at  $w = 16.0\%$  with Load as Parameter.
18. Sinkage as a Function of Slip for a 20 inch x 3 inch Wheel in Sandy-Loam at  $w = 16.0\%$  with Load as Parameter.
19. as a Function of Slip in Sandy-Loam at 16% Moisture Content.
20. Superposition of Pressure Distribution Diagrams Under a 20 inch x 3 inch Wheel in Sandy-Loam at  $w = 16.0\%$  with 50 pound Axial Load.
21. Superposition of Normal Pressure Distribution Diagrams under a 20 inch x 3 inch Wheel in Sandy-Loam at  $w = 16.0\%$  with 100 pound Axial Load.
22. Superposition of Normal Pressure Distribution Diagrams under a 20 inch x 3 inch Wheel in Sandy-Loam at  $w = 16\%$  with 150 pound Axial Load.
23. Equilibrium of the Vertical Forces for a 20 inch x 3 inch Wheel in Sandy-Loam at  $w = 16\%$ .

OBJECTIVE

Measure and analyze pressure distribution and slip sinkage relationships under rigid wheels in various types of soils.

## INTRODUCTION

This paper summarizes current progress of work done under project "Pressure Distribution Beneath a Rigid Wheel" since publication of Land Locomotion Report No. 74 in April 1962.

From Report No. 74, it becomes evident that for the solution of equilibrium equations for wheels, knowledge of the magnitude and position of the ground reaction is essential. This information furnishes the key for the evaluation of wheel sinkage, drawbar-pull and motion resistance. However, at present no exact equation exists for the description of pressure distribution under wheels.

The well known Bekker equation<sup>1</sup> is an estimate of pressure distribution which produces satisfactory results at small sinkages and at a limited number of slip conditions, but at high slip rates and for greater sinkage conditions in sand, for example, this equation introduces an error due to the improper location of the resultant of the pressure distribution. In Land Locomotion Mechanics one must deal with wide ranges of slip and sinkage conditions. A more complete pressure distribution function producing greater accuracy is desirable.

Published data available in this area can be divided into two groups:

1. Pressure transmitted from wheel to soil is measured by "pressure transducers" at certain depths and locations in the soil mass<sup>2,3,4,5</sup>. The disadvantage of this method lies in the difficulty of positioning the pressure cells in the soil. Also, under load from the consolidation process these transducers can move; therefore, such measurements may be erratic.

2. Pressure distribution is measured at the interface contact of wheel and soil by "pressure cells" embedded in the wheel's perimeter<sup>6,7,10</sup>. Using this type of measuring technique, the complete contact pressure can be obtained, which ultimately permits treatment of the wheel as a free body.

Most of these measurements, except those contributed by Vincent and the author, were performed using pneumatic tires. Although the use of pneumatic tires seems more practical from a Land Locomotion standpoint, the rigid test wheel considerably simplifies the analysis of pressure distribution, since no changes in wheel geometry have to be accounted for. However, upon successful completion of the rigid wheel study it is intended to extend the scope of this work to include pneumatic tires.

To the author's knowledge, none of the references quoted except Reference 10 have considered pressure and sinkage measurements in terms of wheel slip-sinkage and in terms of the effect of wheel geometry in different types of soil.

The experimental results reported in this work were intended to develop the following information:

- a. True shape of normal pressure distribution.
- b. Effect of wheel slip on normal pressure distribution.
- c. Effect of wheel-slip on sinkage.
- d. Magnitude of frictional forces on a powered wheel.
- e. Effect of soil properties on pressure distribution, wheel slip-sinkage characteristics, and frictional forces.

#### THEORETICAL BACKGROUND

Definition of forces acting on a Rigid Wheel.

The view is taken here, that once the magnitude and position of the ground reaction is known, the force system acting on the wheel is completely defined. Figure 1 shows the concept of a force system acting on any wheel:

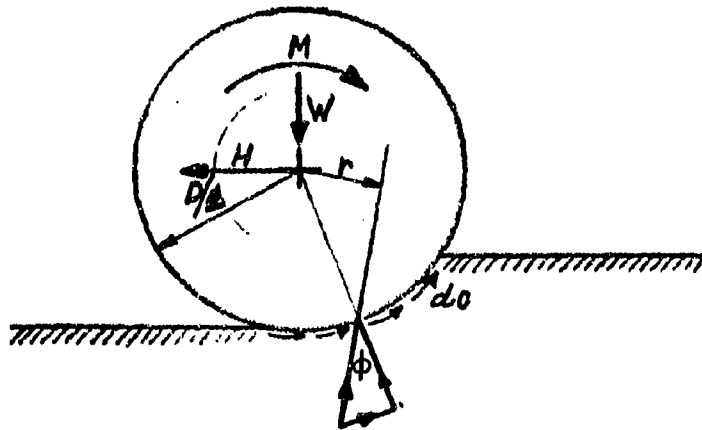


Figure 1

Under the action of an imposed driving moment ( $M$ ), the wheel will have the tendency to slide relative to the ground. The shearing forces ( $t_s$  and  $c$ ) on the contact surface will oppose this motion. From geometry, the normal force ( $N$ ) passes through the center of the wheel. However, by adding  $t_s$  to  $N$ ,  $R$  must act at  $\phi$  relative to the normal when wheel slip or soil failure occurs.

Two possible and different angles of friction can enter into the above problem:

1. The angle of internal friction of the soil.
2. The angle of friction between the wheel and soil.

The smaller of these two angles will determine  $\phi$ . The wheel load ( $W$ ) and the drawbar load ( $H$ ) are taken to act at the center of the hub. It is assumed that the coefficient of friction is constant along the wheel contact length and that the frictional forces act in a direction opposite to the motion. If the contact surface is not too great, it is safe to assume that the ground reaction ( $R$ ) will be tangent to a circle of radius  $r = \frac{D}{2} \sin \phi$  which is commonly called the friction circle in soil mechanics.<sup>8</sup>

The equilibrium equation written on the basis of the concept presented here cannot be solved unless an appropriate pressure distribution function is known. The general equations pertaining to driven, braked and towed wheel conditions have appeared previously in several references<sup>9, 10, 11, 12;</sup> therefore, they will be omitted from this paper.

### TEST FACILITIES AND PROCEDURES

In order to obtain actual pressure distribution curves for rigid wheels under variable loading, slip and soil conditions, a special apparatus was built, Figure 2. The test apparatus consisted of two test wheels: 20 in. x 3 in. and 20 in. x 5 in. A torque meter was attached to the axle of the wheels.

Strain gauge types of "pressure transducers" were embedded in the wheel's perimeter: one at the center of wheel and two close to the edges. This arrangement permitted the pressure distribution measurement laterally as well as longitudinally. The transducers were constructed so that only pressure normal to the wheel would be measured.<sup>7</sup> The wheel was mounted on a dynamometer carriage. A distributor was attached to the drive shaft of the wheel which produced a signal at  $\sqrt{3}^{\circ}$  of angular rotation of the wheel. The linear displacement of the wheel was measured by means of a micro-switch attached to the driving sprocket of the carriage. Therefore, knowing the angular and linear displacements, the slip was easily evaluated.

The wheel was loaded in 50 lb. increments from 50 to 200 lbs. The wheel sinkage was measured by means of a potentiometer connected between the loading tray and the carriage. The pressure cells, micro-switches, potentiometer and the torque meter were connected to a series of analyzers and to a "six-channel" recorder. The recorder continuously recorded the pressures acting against the moving wheel, the exact location of the pressure transducers, the magnitude of angular and linear displacement, torque and sinkages. The pressure cells were calibrated by a device developing a known air pressure and having a maximum capacity of 20 psi,

Figure 3.

Tests were performed in sand and in sandy-loam under laboratory conditions. The soil bin used for this investigation was 40 ft. x 5 ft. x 2 ft. in its overall dimensions and was equally divided between sand and sandy-loam. During test, the sand was kept air-dry. However, in the case of the sandy loam, water was added after each complete experiment as needed to investigate the effect of soil consistency on pressure distribution and slip-sinkage relationship.

Some important characteristics of the materials tested are tabulated in Table I.

In addition to the data in Table I, a grain size distribution diagram for sand is shown in Figure 4.

Atterberg Limits pertaining to sandy-loam are tabulated in Table II:

TABLE II.

Liquid Limit	-	19%
Plastic Limit	-	15%
Plasticity Index	-	4%

Prior to each test run, the dry sand was leveled with a leveling board attached to the carriage in order to assure a reference surface for sinkage measurements. Then the wheel was loaded and the experiment was begun by driving the wheel and tow-carriage simultaneously. Drag was applied to the carriage causing the carriage to slow down relative to the wheel and produce a certain magnitude of slip. By increasing the drag on the carriage, pressure distribution measurements and slip-sinkage measurements at higher slip were possible. This technique was employed for testing at different slips, since speed of carriage and wheel cannot be controlled separately. During this procedure, pressure distribution, angular

TABLE I

SOIL	Moisture Content, $\gamma^*$		Bulk Density ( $\text{lb}/\text{ft}^3$ )*		Angle of Internal Friction $(\phi)^{**}$	Cohesion $c(\text{psi})^{**}$
	(Test)	(Standard Deviation)	(Test)	(Standard Deviation)		
Sand	0.11	0.003	105.70	0.86	36.0	0.10
Sandy-loam Mix No. 1	4.9	0.059	90.72	1.22	--	--
Sandy-loam Mix No. 2	6.5	0.035	88.33	0.84	35.0	0.25
Sandy-loam Mix No. 3	9.1	0.042	87.25	1.24	33.0	0.45
Sandy-loam Mix No. 4	16.0	0.061	103.00	1.00	32.0	0.53

\*Quantities represent the mean and standard deviation of ten randomly selected soil samples.

\*\*Data obtained from direct shear test.

displacement, linear displacement, torque and sinkage data were recorded continuously. The experimental technique produced data which permitted plotting of normal pressure distribution, sinkage and torque as a function of slip between 0 and 100% for each type of soil and loading condition.

The test procedure for sandy-loam was essentially the same as for sand. The only difference existed in processing the material. Sandy-loam was mixed at each test run and at each addition of water content with a Rotary-Tiller. Then it was raked until a smooth soil surface was obtained. After this procedure, two passes with a smooth roller, weighing 200 lbs., were applied. Although this resulted in an increase of soil density, it assured a more uniform soil structure, which is demonstrated by the fact that the deviations from the mean in moisture and density values are within acceptable limits. As a matter of interest, it should be noted here that deviation from mean density at least doubled when the roller passes were omitted.

### TEST RESULTS

The results of driving moment, pressure distribution and slip-sinkage measurements are presented in diagrams and chart forms.

Figure 5, shows a typical torque versus slip relationship with wheel load as parameter in dry sand. This figure also confirms that for slip conditions in sand in excess of 30% the assumption that  $\phi$  is constant is valid. If shear strength is taken as independent of depth, the torque versus slip relationship depicted can be considered as a shear deformation diagram since torque is proportional to the tangential forces and slip to the corresponding deformations. The peak points of these curves were taken for the construction of the Mohr-Coulomb envelop, and the value of  $\phi$  was found to be very nearly equal to that determined by sliding friction experiments. The sliding friction experiments resulted in  $\phi = 24^\circ$  and  $c = 0$  while evaluating those from torque-slip relationship when the normal pressures at wheel-soil contact are known, gave  $\phi = 23^\circ$  and  $c = 0$ .

Actual normal pressure distribution diagrams are shown in the next series of figures. Figure 6 illustrates the pressure distribution in sand as a function of the polar angles under a 20 in. x 3 in. wheel at various loads. The slip is held constant at 0%. The effect of slip on pressure distribution is shown in Figure 7, when the soil (sand), wheel size and wheel load are kept constant.

It is apparent from the latter two pressure distribution diagrams that as slip occurs, pressure distribution as well as sinkage become a function of slip. An increased sinkage develops higher motion resistance; therefore, the resultant of the pressure distribution will have a higher angle of inclination relative to the vertical.

Another important factor is that the pressure distribution extends beyond the point of maximum sinkage. The extent of pressure distribution to the trailing portion of the wheel is about  $10^{\circ}$  or less from the toe of the wheel in most of the pressure profiles reported here. This phenomenon can be attributed to the flow of the material into the wheel rut in sands, to the rebound of the material in firm soils.

Note that the pressure distribution in the lateral direction is also shown in the figures. Dots denote the pressure at the center of the wheel and crosses denote the pressure close to the edges of the wheel. The pressure transducers mounted at the edges of the wheel were averaged on the recording device so that the crosses represent the average value of the pressure on the two wheel edges.

Figure 8, shows the same information for a 20 in. x 5 in. wheel as was shown in Figure 7 for the 20 in. x 3 in. wheel in sand. The variation in pressure across the wheel face is very significant indeed for this wheel. The pressures at the center of the wheel were found approximately twice as high, as they were observed close to the edges of the wheel. In case of the narrow wheel, the variation of pressure in the lateral direction is negligible except for those pressure distribution diagrams which were obtained at very high slip condition.

Figure 9 further illustrates the importance of the lateral pressure distribution for wide wheels. Pressure is shown as a function of polar angles for specific cases of slip under a constant load.

The next two figures, Figures 10 and 11, show sinkage (maximum vertical deformation) as a function of slip in sand for the 20 in. x 3 in. and 20 in. x 5 in. wheel, respectively. Again, it is apparent that as slip occurs sinkage

rapidly increases. For sand the compaction effects are small, so that the wheel can dig itself into the ground. This process is associated with slip failure in which the wheel removes material from the contact surface and deposits it behind the wheel.

The next figure, Figure 12, shows sinkage as a function of the angle of inclination of the resultant of normal pressures in sand for both wheels tested. This function may be approximated by a straight line having the following equation:

$$z_0 = 6.87 \theta$$

After some manipulation it may be seen that in sand the normal resultant divides the ground contact arch approximately into two equal parts, thereby confirming the hypothesis of Tanaka<sup>12</sup> who assumed in general that the angular position of the resultant ( $N$ ) is half that of the angle of sinkage.

If the vertical component of the ground reaction is evaluated by graphical integration, a chart plotting  $N_v$  and  $R_v$  against  $W$  can be made.  $N_v$  is the vertical component of the normal resultant  $N$ , while  $R_v$  is the vertical component of the resultant of normal and frictional forces. It is found that  $N_v$  alone does not satisfy the equilibrium of the vertical forces. This indicates that frictional forces must be included to achieve equilibrium. The frictional forces were evaluated from Coulomb's equation for maximum shear stress. The agreement obtained by the inclusion of the frictional forces is shown in Figure 13, and it can be seen that the magnitude of the discrepancy is within an acceptable limit.

The tests were continued to investigate the behavior of the wheel in a sandy loam at various moisture contents.

The following illustrations refer to results obtained. Figures 14, 15, 16, and 17, show slip-sinkage relationship for a 20 in. x 5 in. wheel in sandy loam Mix No. 1 -Mix No. 4. Figures 14 and 15 show mixes which represent sandy loam at low, 4.9% and 6.5% of moisture content, respectively. The slip-sinkage relationship is very similar to those obtained in sand. However, at 9.1% and 16% moisture content, sinkage will be independent of slip. Similar results were obtained with a 20 in. x 3 in. test wheel at 16% moisture content. This relationship is shown in Figure 18.

An explanation of slip-sinkage behavior of wheels in sand and in sandy loam may be given as follows: in granular soils (dry sand and sandy loam at low moisture content) the compaction effects are very small. Therefore, a "soil transport" phenomenon exists underneath the wheel. With added water and the same compactive effort of roller and wheel, greater density can be obtained up until the water content reaches the value where maximum density is achieved. The sandy loam type of soil is highly compactable at higher moisture contents. Movement of the moisture to the wheel soil interface serves as a lubricant; therefore, the transport of soil by wheel does not occur.

These series of slip-sinkage tests were performed with the aim of pinpointing the minimum amount of cohesion at which sinkage may be taken as independent of slip.

From the experiments, it appears that the cohesive properties of soils are responsible for the dependence or independence of sinkage upon slip. The number of experiments conducted suggests that above 0.5 psi of cohesion sinkage may be regarded as independent of slip.

Figure 19, shows the angular position of the resultant of the normal pressure distribution as a function of slip for a 20 in. x 3 in. wheel in sandy loam at 16% of moisture content. This curve also shows the independence of  $\alpha$  and slip.

Since the sinkage and  $\alpha$  were found to be independent of slip, the pressure distribution measurements were presented in a superimposed form. Figures 20, 21, and 22 show the superimposition of all the pressure distribution diagrams regardless of slip at 50, 100, and 150 pounds of wheel load, respectively. These measurements were taken in sandy loam Mix No. 4. Note that the trend of lateral pressure distribution reverses; that is, close to the edges of the wheel higher pressures were recorded than at the center of the contact strip in a cohesive type of soil.

It can be stated again from the experiments that the angular position of the resultant approximately bisects the contact angle.

Similarly, as was shown for sand, equilibrium considerations pertaining to the above normal pressures, estimated frictional forces, and imposed loads are shown in Figure 23. It is seen that the frictional forces must also be included in the description of a wheel operation in a material having cohesion, if equilibrium is to be achieved.

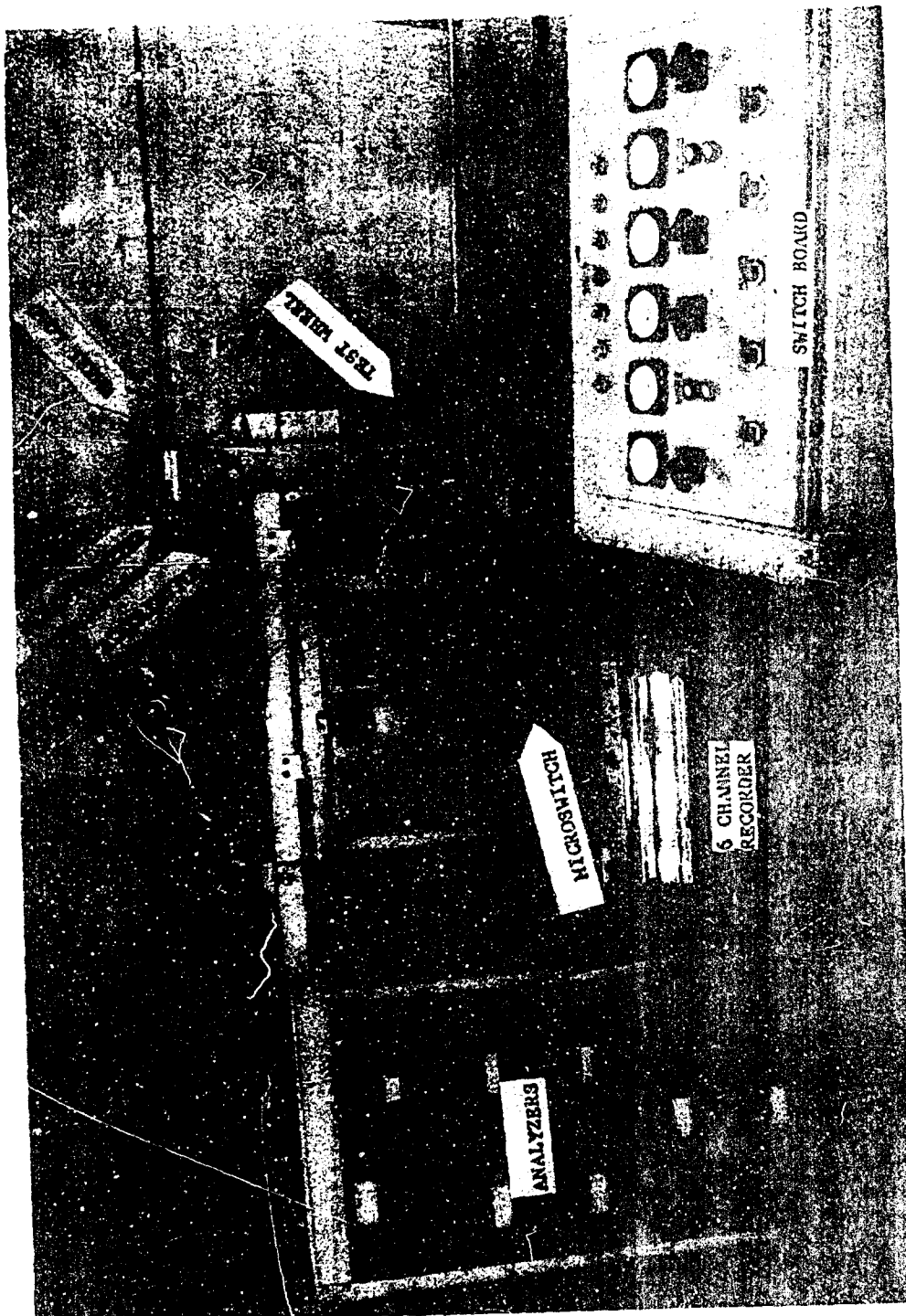
### CONCLUSIONS

1. An analytically correct equation for pressure distribution must include not only soil properties and wheel geometry as it was previously believed, but also the slip-sinkage relationship and tangential forces.
2. The effect of frictional forces are significant and should be included in equilibrium equations for wheels. The frictional forces may be conveniently estimated from Coulomb's equation for maximum shear strength.
3. Sinkage is a function of slip in granular soils; however, in cohesive soils sinkage may be taken independent of slip. Further tests are necessary to confirm this statement, since tests in loam with a moisture content in excess of 16% have not been performed.

### RECOMMENDATIONS

1. It is recommended that in addition to the quantities measured and reported here, drawbar-pull measurements also should be made.
2. It is recommended that further experiments be performed confirming:
  - a. The minimum amount of cohesion necessary to judge sinkage independent of slip.
  - b. Whether or not, above the maximum density, sinkage is independent of slip.

BEST AVAILABLE COPY

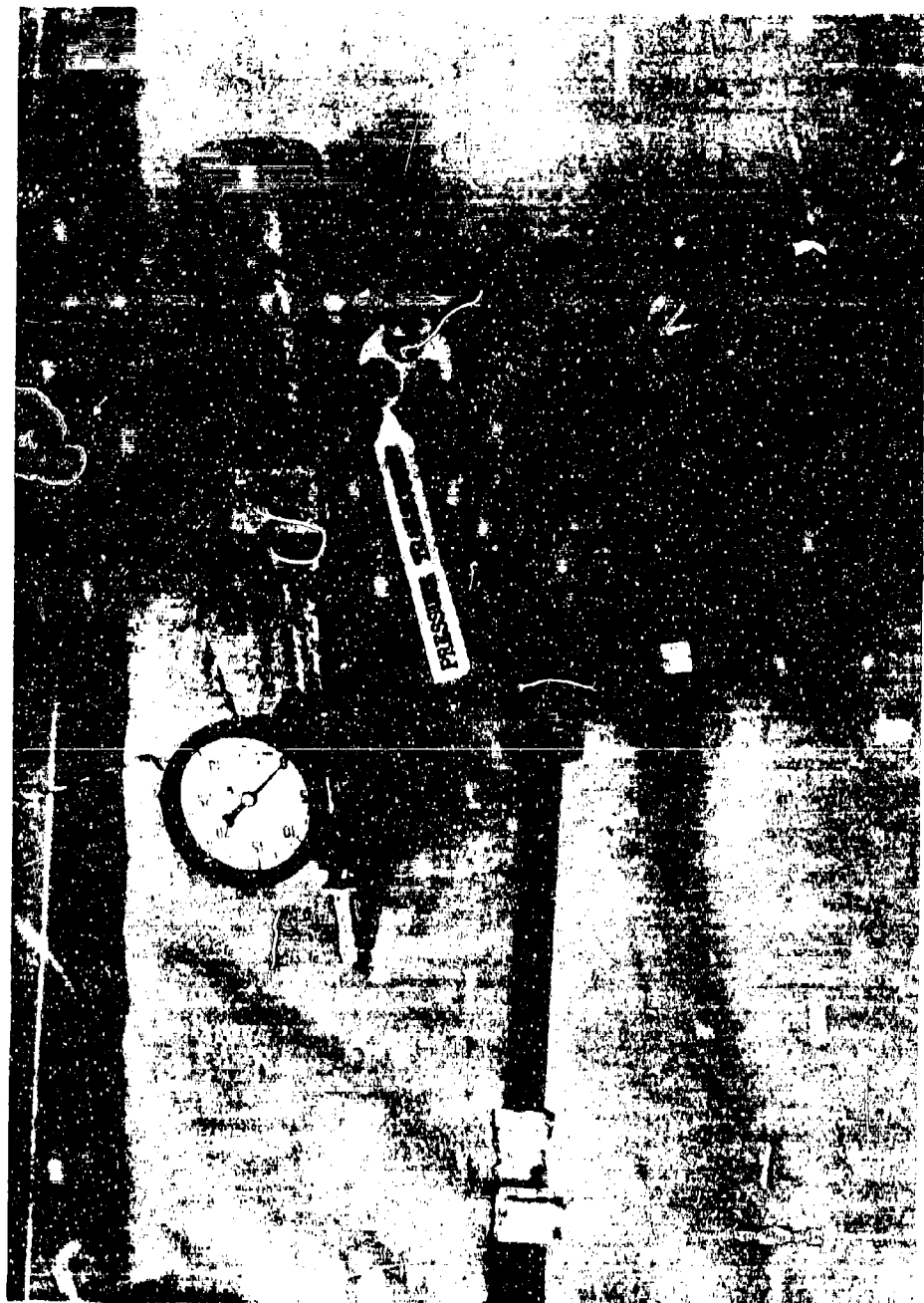


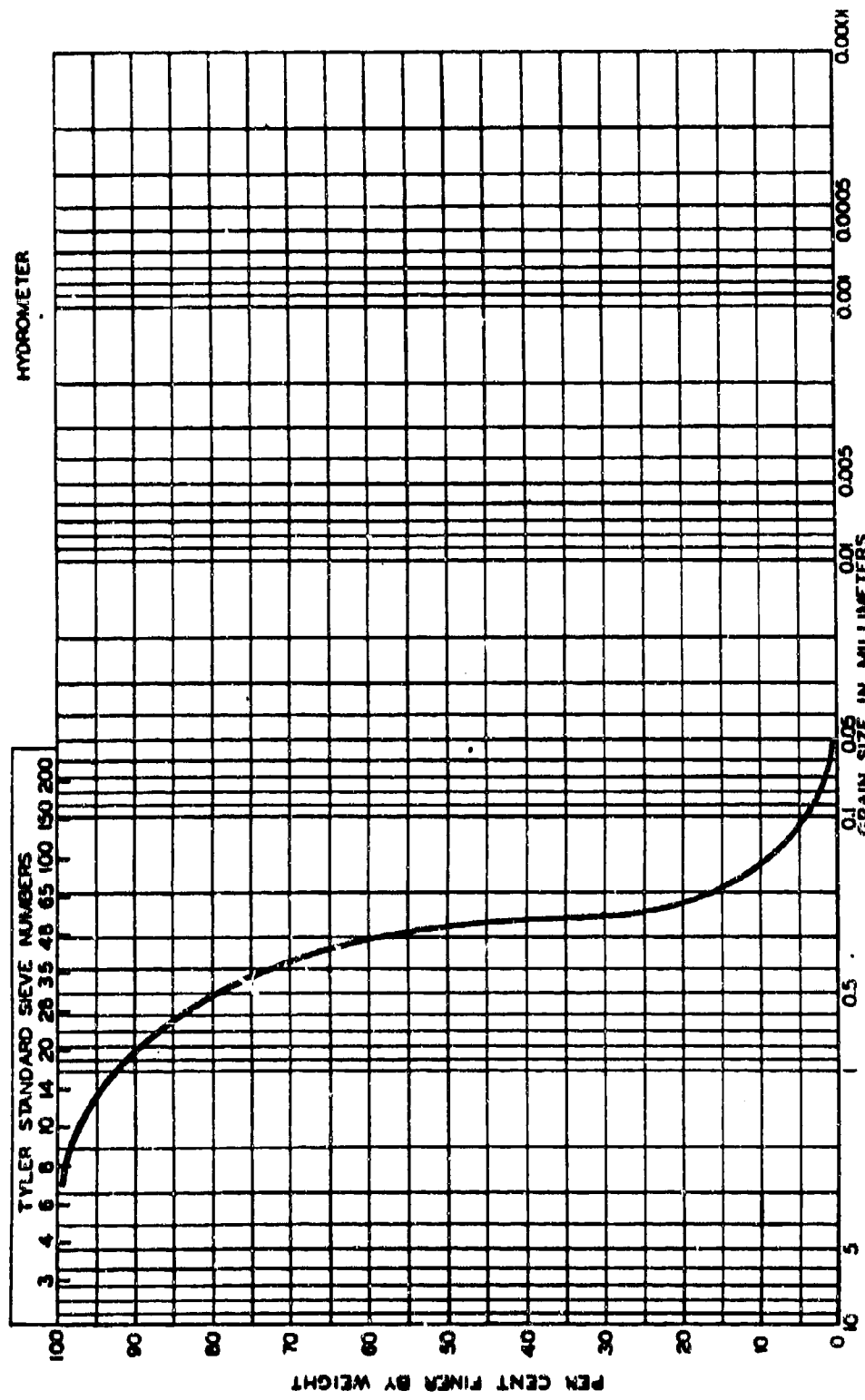
TEST APPARATUS

Figure 2

CALIBRATION OF THE LOAD CELLS BY AIR PRESSURE

Figure 5



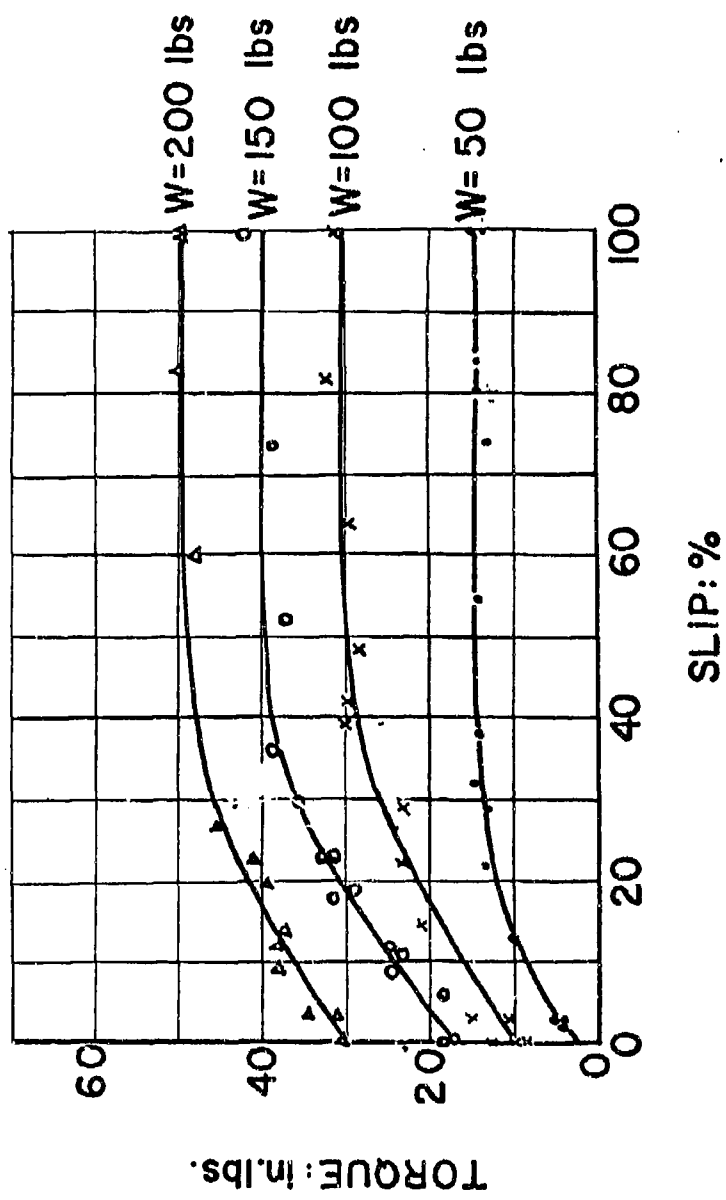


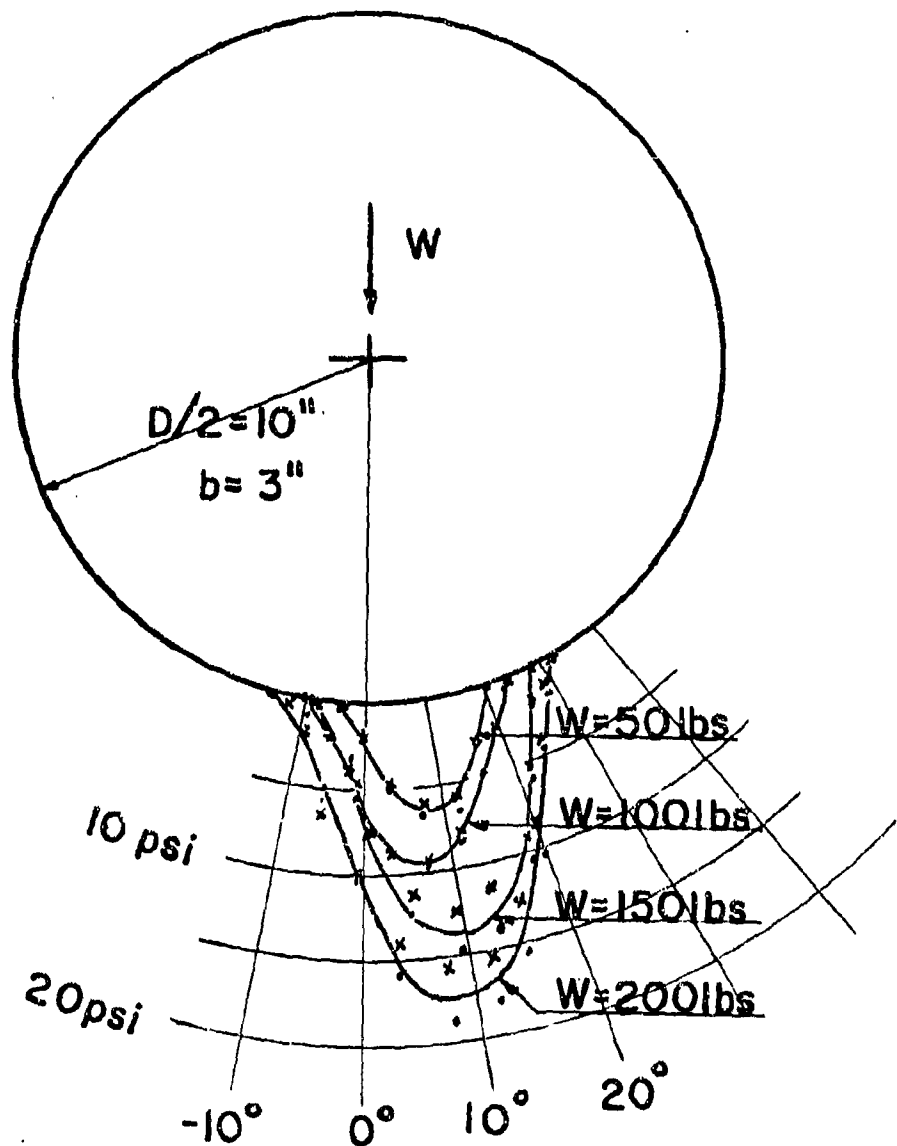
GRAIN SIZE DISTRIBUTION DIAGRAM FOR SAND

Figure 4

TORQUE AS A FUNCTION OF SLIP WITH LOAD AS PARAMETER IN DRY SAND

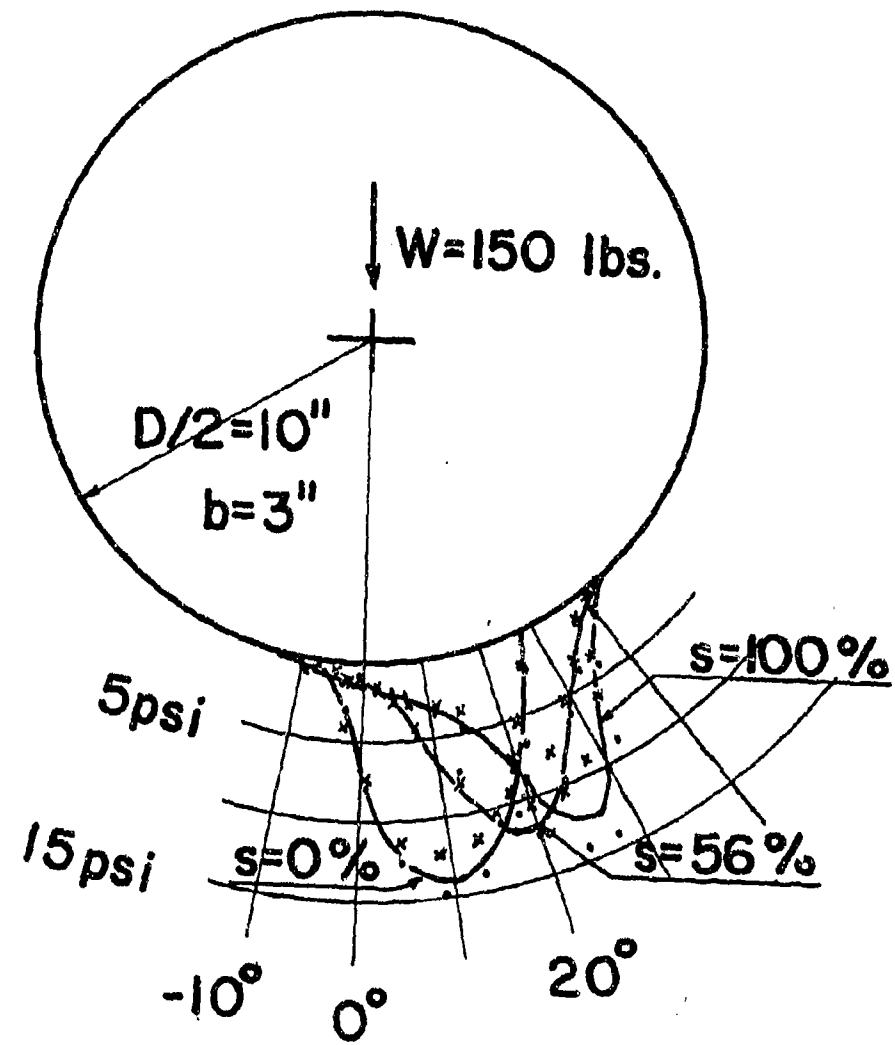
Figure No. 5





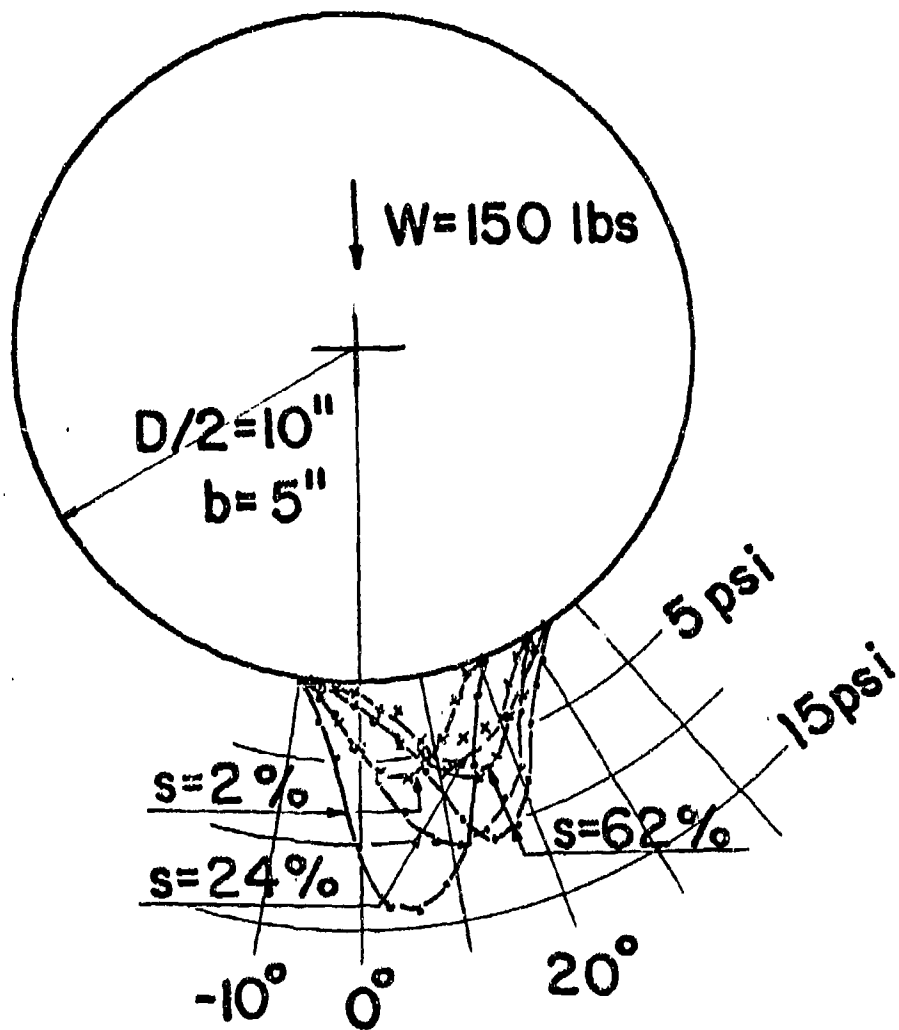
NORMAL PRESSURE DISTRIBUTION FOR DIFFERENT  
WHEEL LOADS IN SAND AT NO SLIP.

Figure No. 6



EFFECT OF WHEEL SLIP ON PRESSURE DISTRIBUTION  
UNDER A 20" x 3" WHEEL IN SAND.

Figure No. 7

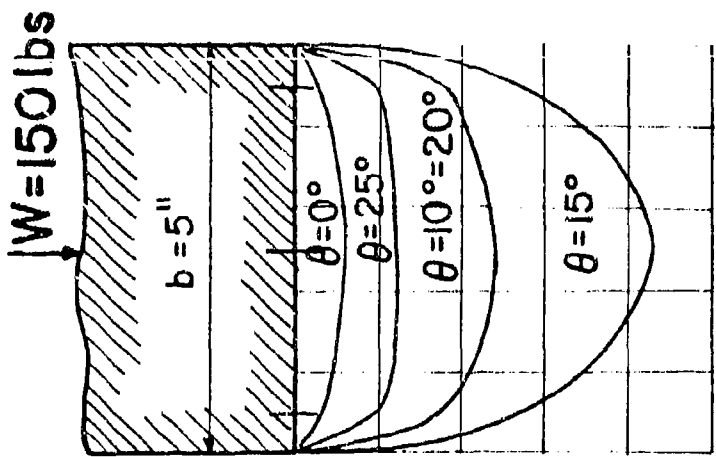


EFFECT OF WHEEL SLIP ON PRESSURE DISTRIBUTION  
UNDER A  $20'' \times 5''$  WHEEL IN SAND.

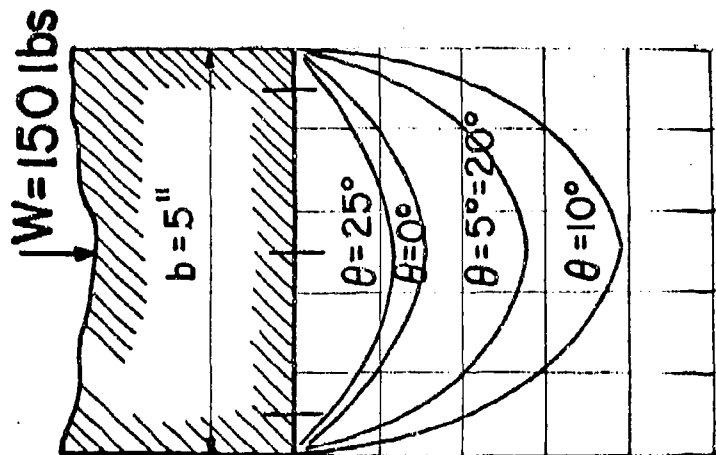
Figure No. 8

FIGURE NO. 9  
VARIATIONS OF LATENT PRESSURE DISTRIBUTION IN SAND FOR  
LATENT PRESSURE DISTRIBUTION IN SAND FOR

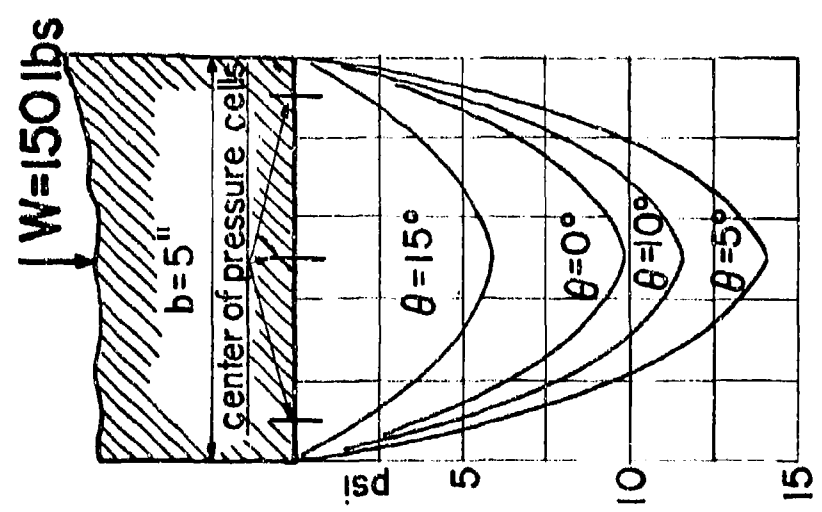
$s = 62\%$



$s = 24\%$

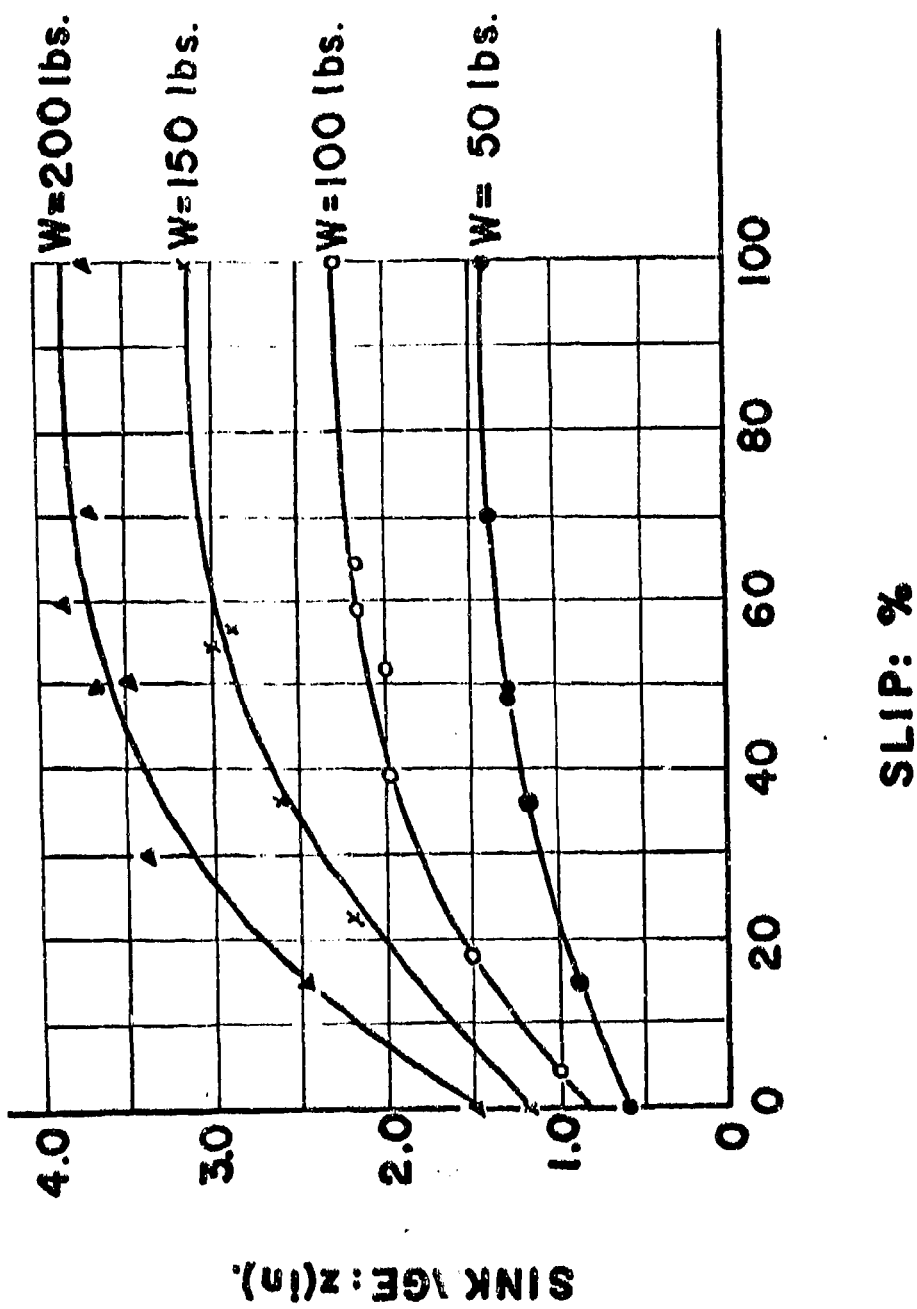


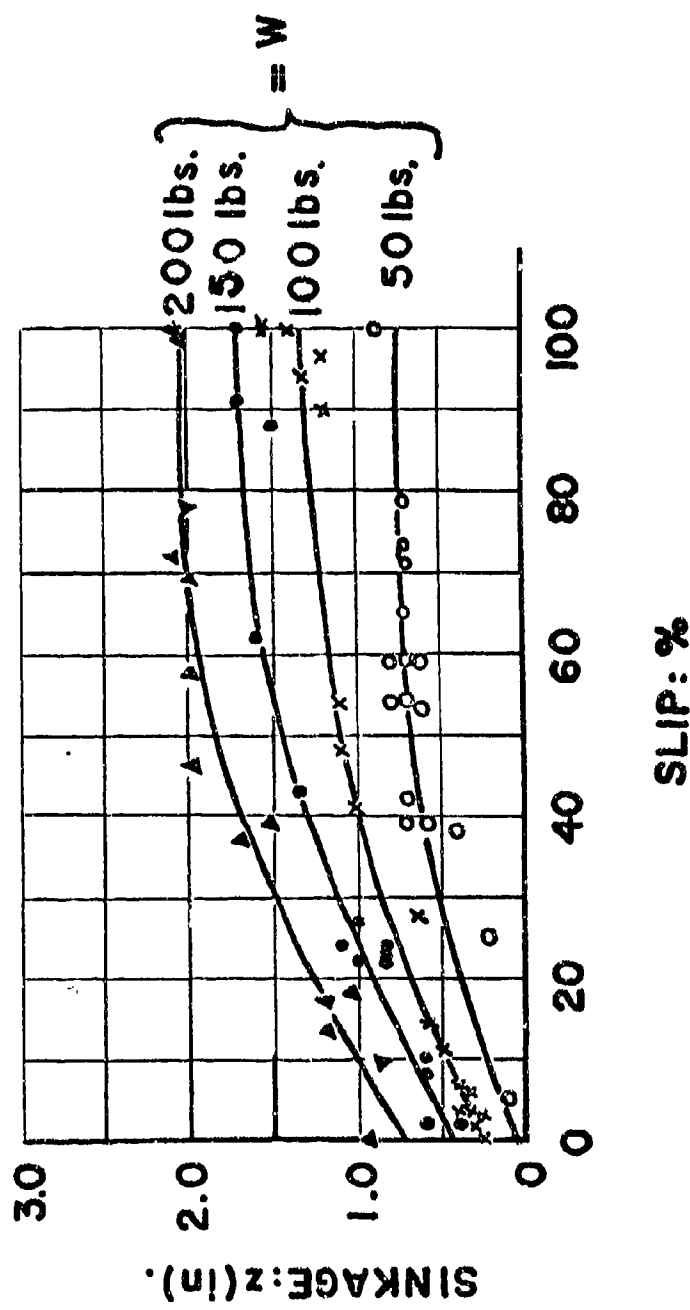
$s = 2\%$



SINKAGE AS A FUNCTION OF SLIP FOR A 20x3 in. WHEEL IN SAND WITH LOAD AS PARAMETER.

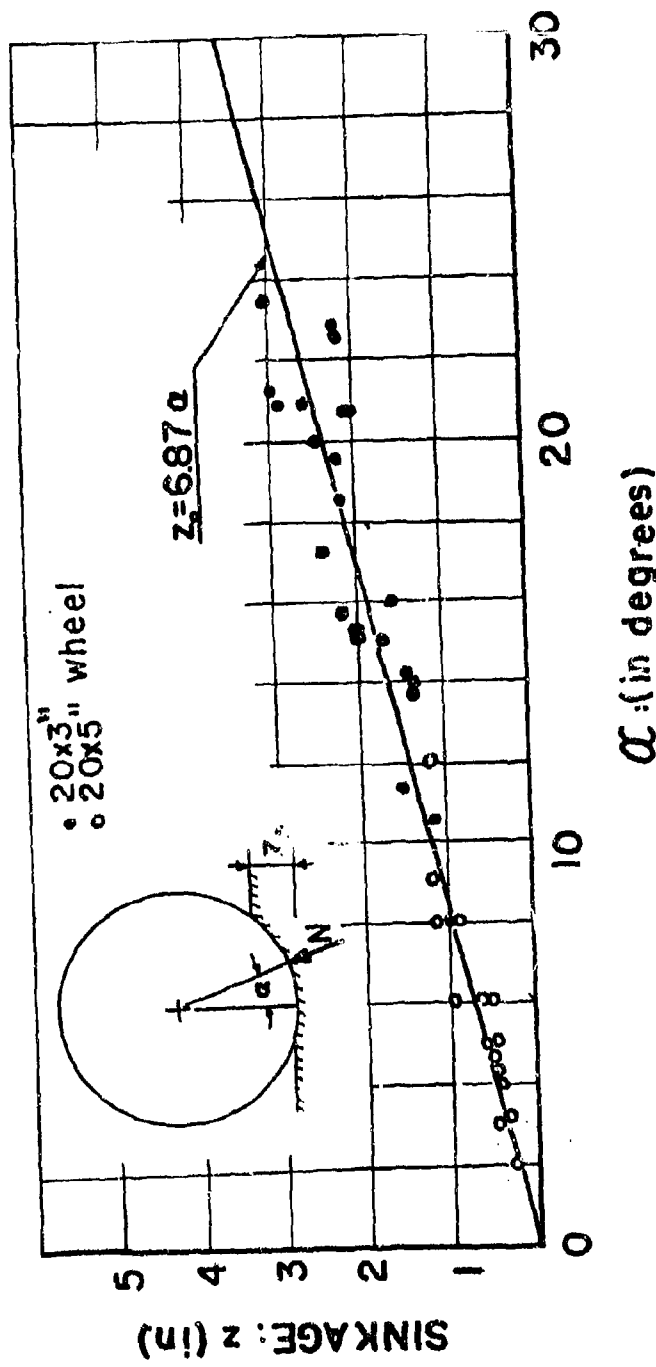
Figure No. 1c





SINKAGE AS A FUNCTION OF SLIP FOR A 205 in. WHEEL IN SAND WITH LOAD AS PARAMETER.

Figure No. 11



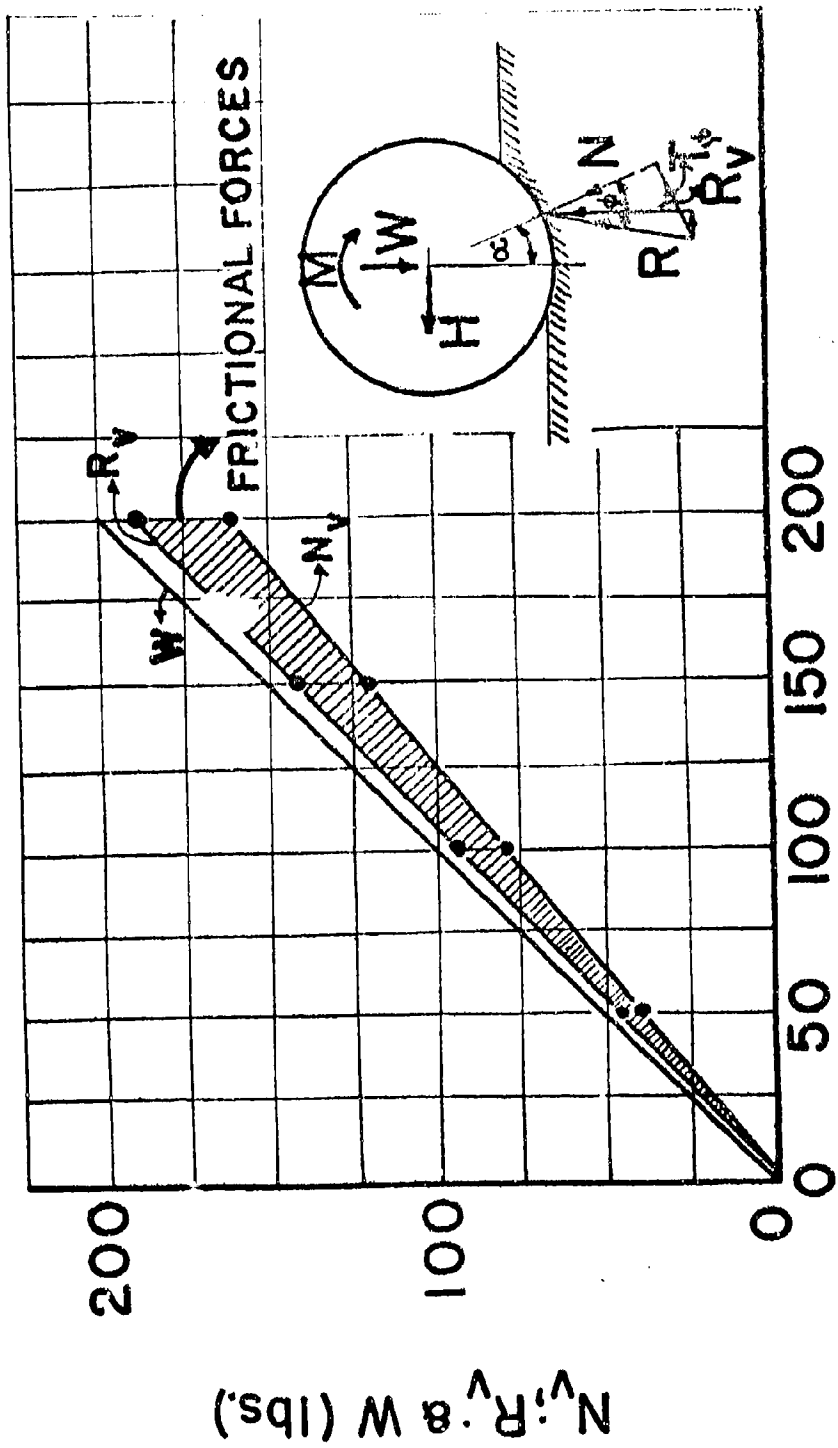
SINKAGE AS A FUNCTION OF THE ANGLE OF  
 INCLINATION OF THE NORMAL REACTION,  
 $\alpha$  : (in degrees)

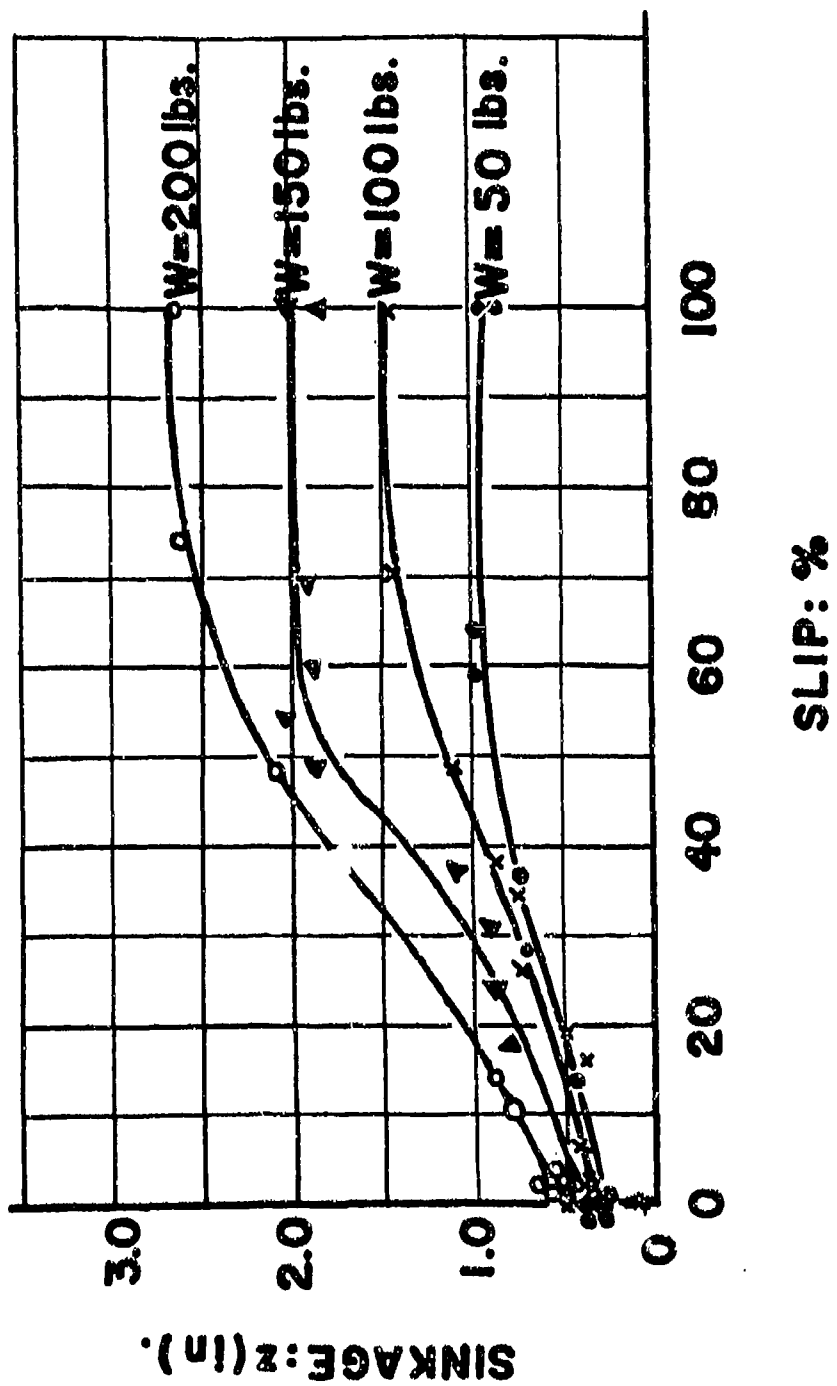
Figure No. 12

## AXIAL LOAD: W (lbs.)

EQUILIBRIUM OF THE VERTICAL FORCES FOR 20x3" WHEEL IN DRY-SAND.

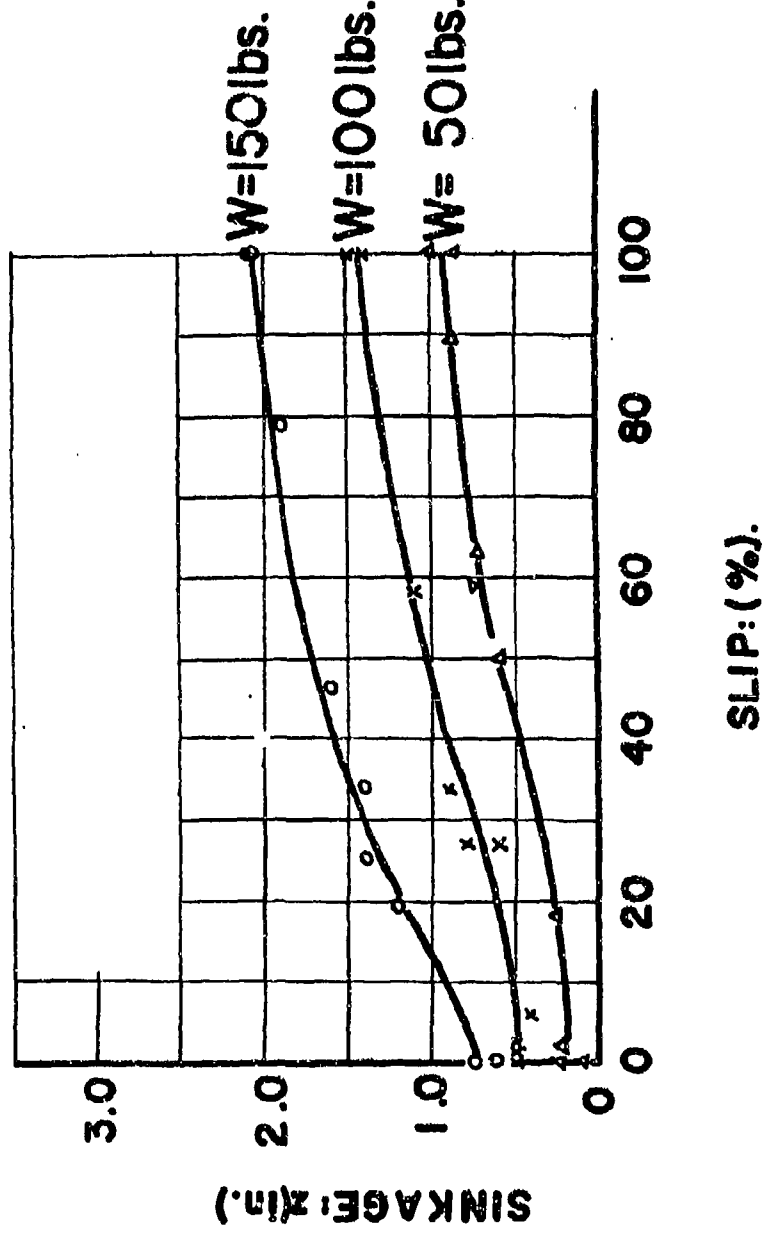
Figure No. 13





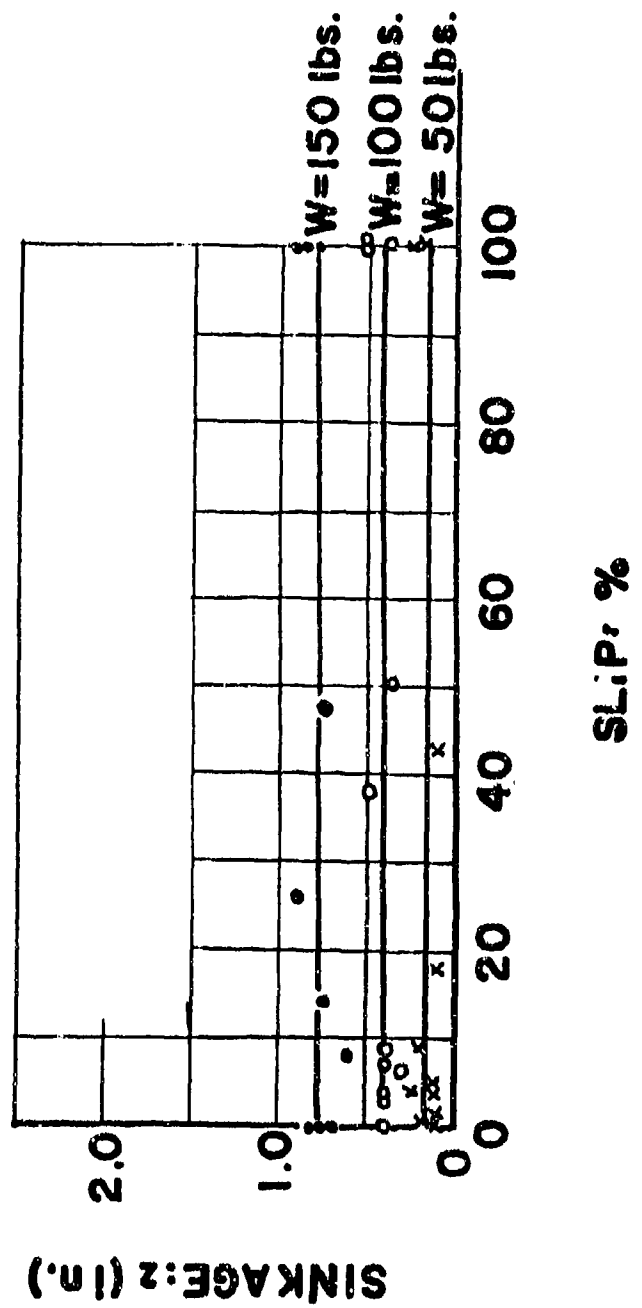
SINKAGE AS A FUNCTION OF SLIP FOR A 20x5" WHEEL IN SANDY-LOAM AT  $W = 4.9 \text{ ft}^2/\text{lb}$  LOAD AS PARAMETER.

Figure No. 14



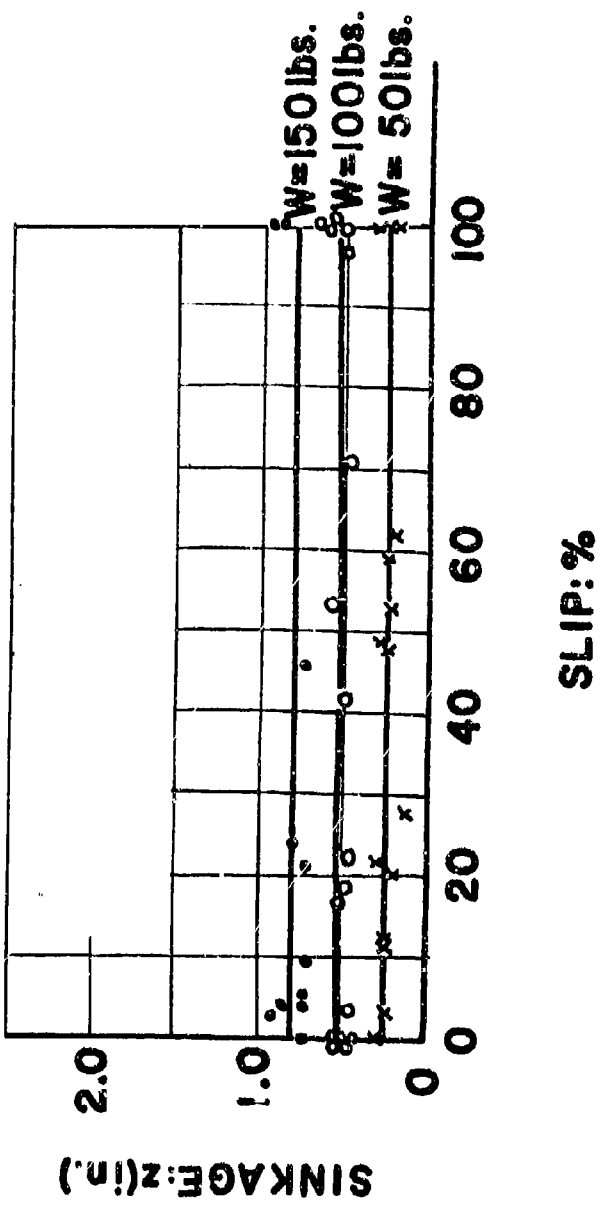
SINKAGE AS A FUNCTION OF SLIP FOR A 22x5" WHEEL IN SAND-LOAD AT 6.5% STATIC LOAD AS PARAMETER.

Figure No. 15



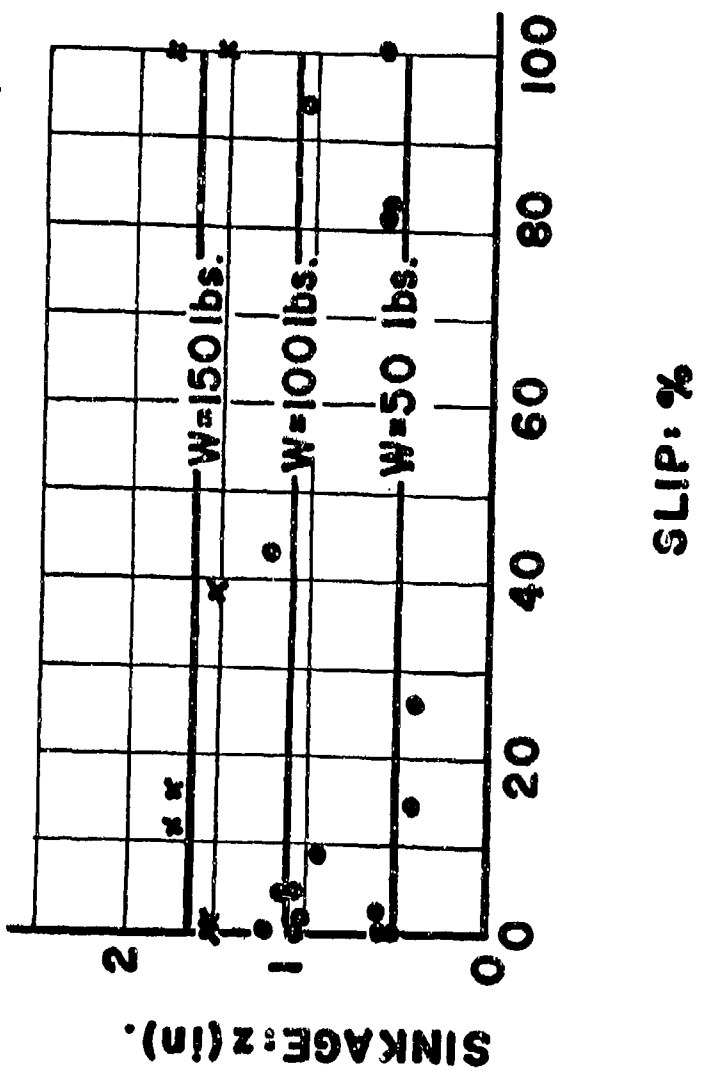
SINKAGE AS A FUNCTION OF SLIP FOR A 20x5" WHEEL IN SANDY-LOAM AT  $n=9.1\%$  WITH LOAD AS PARAMETER.

Figure No. 16



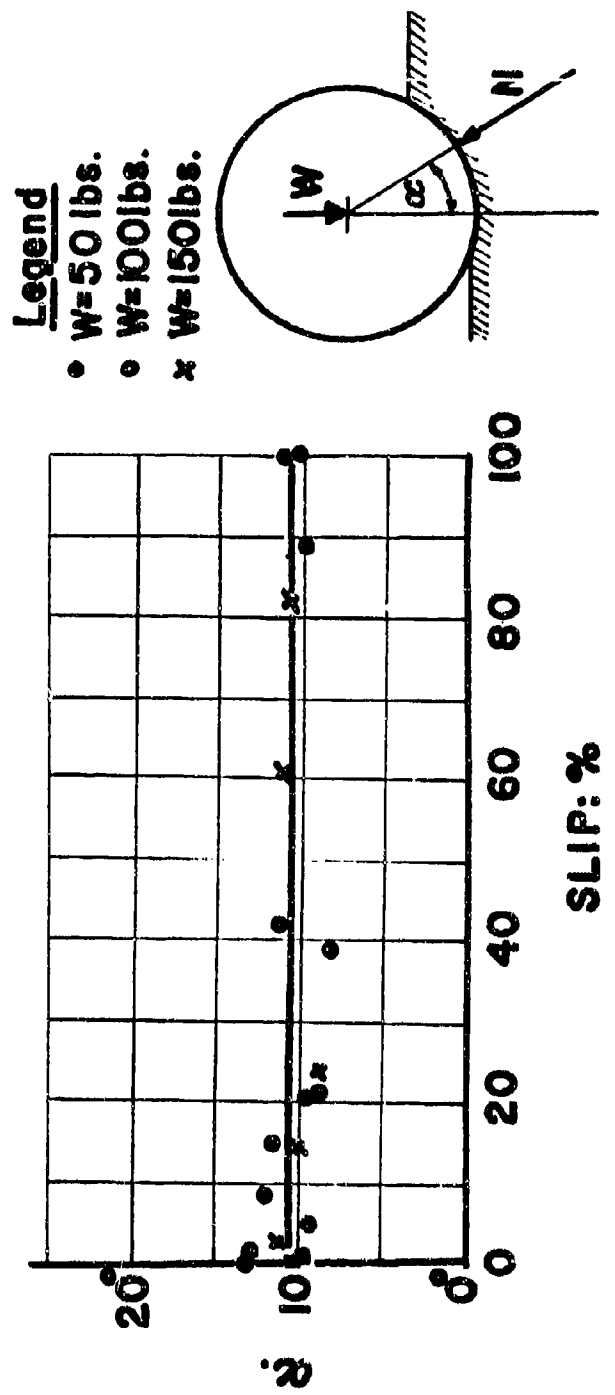
SINKAGE AS A FUNCTION OF SLIP FOR A 20x5" WHEEL IN SANDY-LOAM AT  $v=16.0$  ft/min LOAD AS PARAMETH.

Figure No. 17



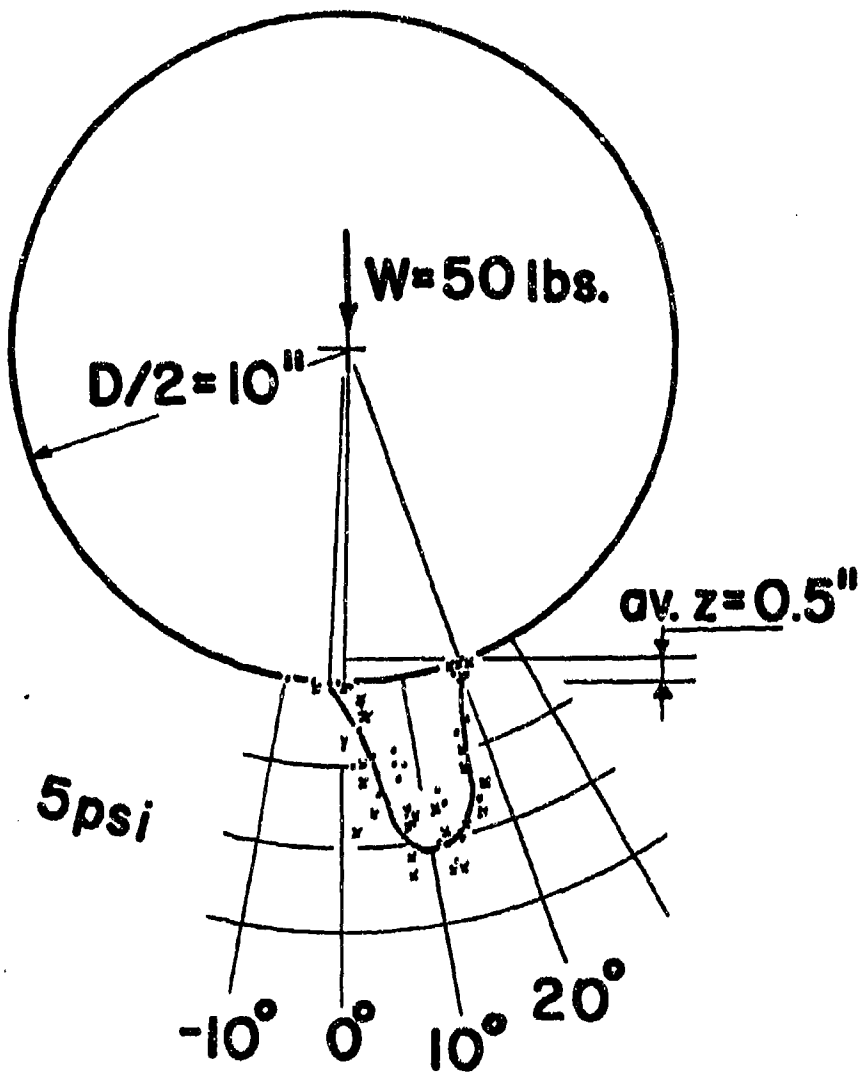
SINKAGE AS A FUNCTION OF SLIP FOR A 20x3" WHEEL IN SANDY LOAM AT  $v=16.0$  ft/min WITH LOAD AS PARAMETER.

Figure No. 18



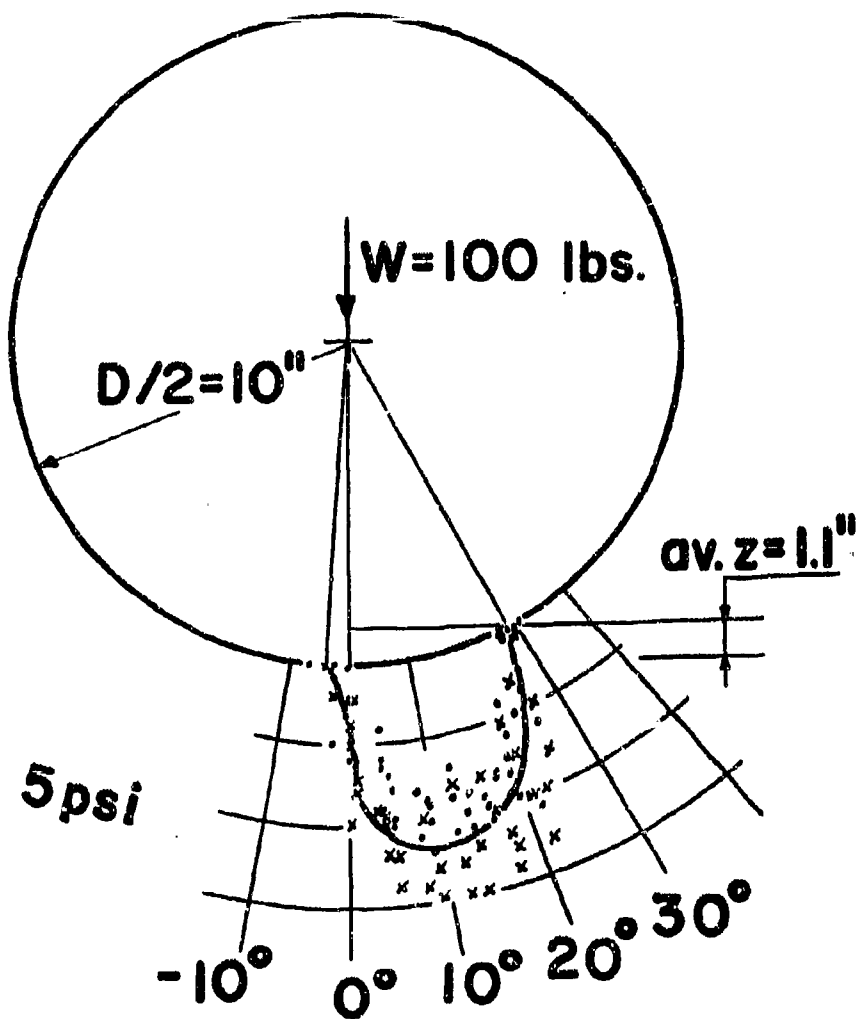
$\alpha$  AS A FUNCTION OF SLIP IN SANDY LOAM AT 14% MOISTURE CONTENT.

Figure No. 19



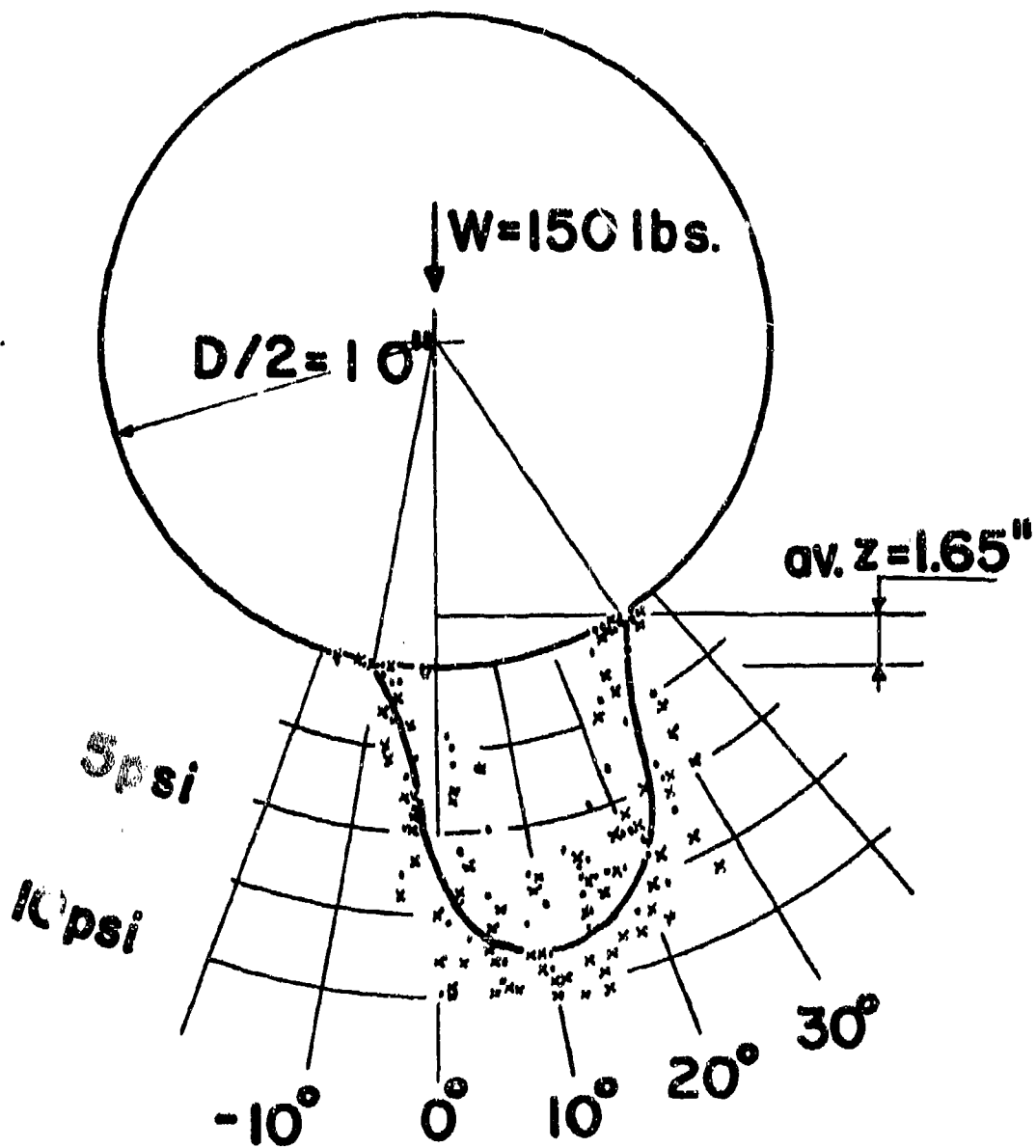
SUPERPOSITION OF PRESSURE DISTRIBUTION DIAGRAMS UNDER A 20x3" WHEEL  
IN SANDY-LOAM AT  $w=16.0\%$  WITH 50 lbs Axial LOAD.

Figure No. 20



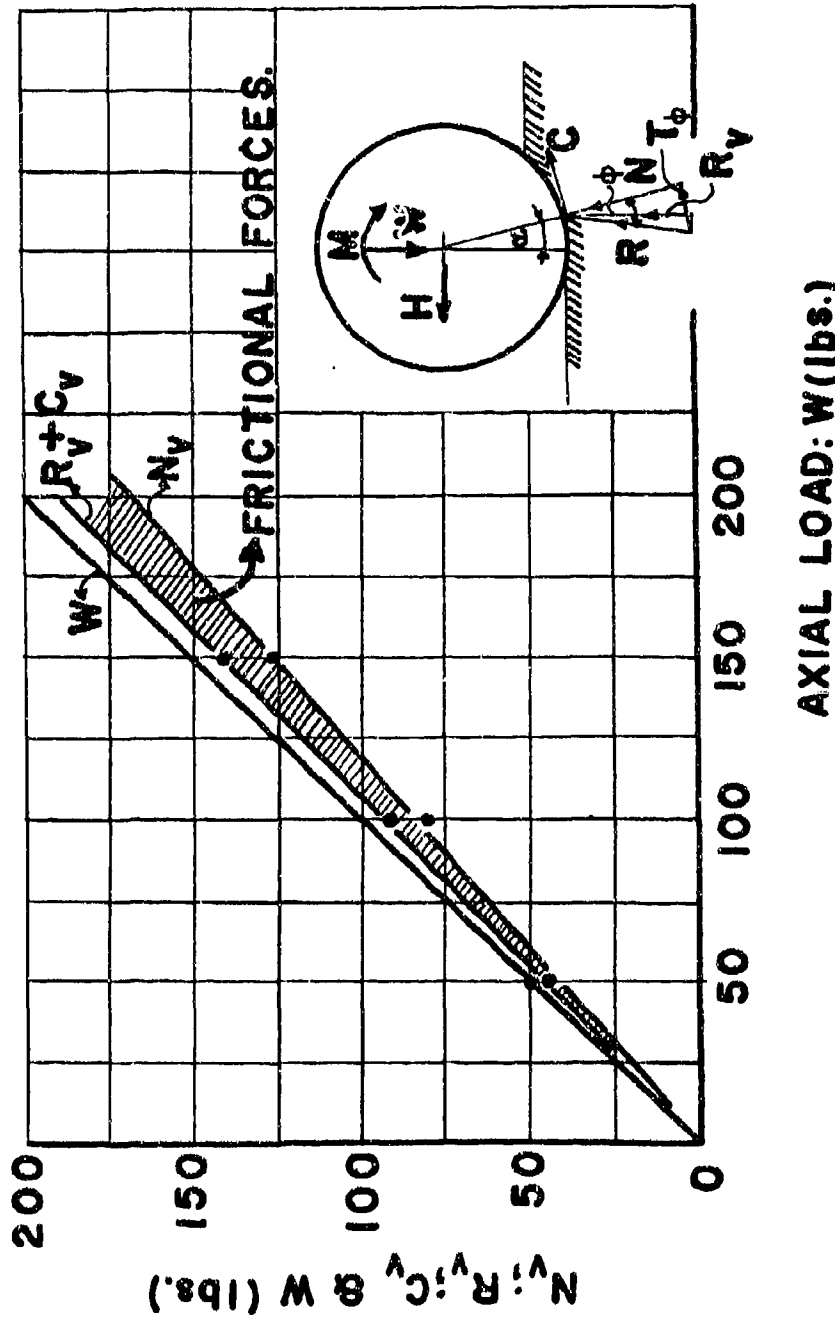
SUPERPOSITION OF NORMAL PRESSURE DISTRIBUTION DIAGRAMS UNDER A 20x3" wheel  
IN SANDY-LOAM AT  $w=16.0\%$  WITH 100 lbs AXIAL LOAD.

Figure No. 21



SUPERPOSITION OF NORMAL PRESSURE DISTRIBUTION DIAGRAMS UNDER A 20x8" WHEEL  
IN SANDY-LOAM AT  $w=16.0\%$  with 150 lbs AXIAL LOAD.

Figure No. 22



EQUILIBRIUM OF THE VERTICAL FORCES FOR A 20x3" WHEEL IN SAND - LOAD AT = 166.

Figure No. 23

REFERENCES

1. Bekker, M. G., "Theory of Land Locomotion", University of Michigan Press, Ann Arbor, 1956.
2. Vandenberg, G. E. and W. R. Gill, "Pressure Distribution Between a Smooth Tire and Soil". ASAE Paper No. 59-108, Ithaca, 1959.
3. Cooper, A. W., G. E. Vandenberg, H. F. McColly, A. E. Erickson, "Strain Gage Cell Measures Soil Pressure", AG.E, Vol. 38, April 1957.
4. Reaves, C. A. and A. W. Cooper, "Stress Distribution in Soils Under Tractor Loads", Ag.E., Vol. 41, Jan. 1960.
5. Schne, W., "The Transmission of Force Between Tractor Tires and Farm Soils", Grundlagen der Landtechnik, 1952.
6. Vincent, E. T., "Pressure Distribution on and Flow of Sand Past a Rigid Wheel", 1st. International Conference on the Mechanics of Soil Vehicle Systems, Torino, 1961.
7. Trabbic, G. W., "The Effect of Drawbar Load and Tire Inflation on Soil-Tire Interface Pressure," M. S. Thesis, Michigan State University, 1959.
8. Capper, L. and Cassie, F., "The Mechanics of Engineering Soils", McGraw-Hill, New York, 1953.
9. Schuring, D., "On the Mechanics of Rigid Wheels on Soft Soil", V. D. I., June 1951.
10. Hegedus, E., "A Preliminary Analysis of the Force System Acting on a Rigid Wheel", Land Locomotion Laboratory, OTAC, Report No. 74, 1962.
11. Phillips, J., "A Discussion of Slip and Rolling Resistance", 1st International Conference on the Mechanics of Soil-Vehicle Systems, Torino, 1961.
12. Tanaka, T., "The Statical Analysis and Experiment on the Force to the Tractor Wheel", 1st International Conference on the Mechanics of Soil-Vehicle Systems, Torino, 1961.